

# Studies on syntheses and properties of novel CeO<sub>2</sub>/polyimide nanocomposite films from Ce(Phen)<sub>3</sub> complex

Zhenping Shang<sup>a</sup>, Changli Lü<sup>b</sup>, Xiaodan Lü<sup>b</sup>, Lianxun Gao<sup>a,\*</sup>

<sup>a</sup> State Key Laboratory of Polymer Physics and Chemistry, Changchun Institute of Applied Chemistry, Chinese Academy of Sciences, Graduate School of Chinese Academy of Sciences, Changchun 130022, PR China

<sup>b</sup> Institute of Chemistry, Northeast Normal University, Changchun 130024, PR China

Received 16 October 2006; received in revised form 23 March 2007; accepted 29 March 2007

Available online 12 April 2007

## Abstract

A series of cerium dioxide (CeO<sub>2</sub>)/polyimide (PI) nanocomposites were successfully prepared from Ce(Phen)<sub>3</sub> and polyamic acid (PAA) via the solution direct-dispersing method, followed by a step thermal imidization process. TGA and XPS studies showed that the cerium complex decomposed to form CeO<sub>2</sub> during the thermal imidization process at 300 °C. SEM observation showed that the formed CeO<sub>2</sub> as nanoparticles was well dispersed in polyimide matrix with a size of about 50–100 nm for samples with different contents of CeO<sub>2</sub>. Thermal analysis indicated that the introduction of CeO<sub>2</sub> decreased the thermal stability of nanocomposite films due to the decomposition of Ce(Phen)<sub>3</sub> in the imidization process, while the glass transition temperature ( $T_g$ ) increased obviously, especially nanocomposite films with high loading of CeO<sub>2</sub> exhibited a trend of disappearance of  $T_g$ . DMTA and static tensile measurements showed that the storage modulus of nanocomposite films increased, while the elongation at break decreased with increasing CeO<sub>2</sub> content.

© 2007 Elsevier Ltd. All rights reserved.

**Keywords:** Polyimide; Cerium complexes; 1,10-Phenanthroline

## 1. Introduction

Incorporation of inorganic materials in polymer matrix can improve the mechanical, thermal, dielectric and optical properties of polymers [1,2]. In recent years, especially, various nanosize inorganic components with high surface area have been used to enhance the performance of polymer materials [3–6]. To achieve the object of high performance for organic/inorganic hybrid composites, there are still many technological challenges to control microstructure and phase separation as well as the interfacial force between organic and inorganic phases [7,8].

Polyimide (PI) as a high-performance polymer materials has been found many important applications in aerospace, advanced microelectronics and other advanced technologies

due to their excellent mechanical, thermal and dielectric properties [9–11]. PI as organic matrix has recently been used to prepare polyimide composites with improved mechanical, thermal and other properties by incorporation of inorganic components. For example, silica/PI [12–14], TiO<sub>2</sub>/PI [15,16], layered silicate/PI [17,18] and metal or metal oxide/PI [19] have been prepared by different methods. Rare earth compounds, involving lanthanum(III) oxide nanoparticles, lanthanide(III) acetate additives, Eu<sub>2</sub>O<sub>3</sub> and Eu<sup>3+</sup> complexes, were also incorporated into PI matrix to prepare hybrid materials [20–24]. These hybrid materials exhibited the enhanced dimensional stability. However, the studies on the rare earth/PI hybrids are relatively less. What effect of the other rare earth from various rare earth ions and ligands on the properties of polymer? It needs more efforts and researches to explore and enrich these contents. As one of the series of researches, we here prepared a new cerium complex with 1,10-phenanthroline(Phen) ligand and introduced it in PI matrix to synthesize a series of CeO<sub>2</sub> nanoparticles/PI nanocomposite

\* Corresponding author. Tel.: +86 431 85697831.

E-mail address: [lxgao@ciac.jl.cn](mailto:lxgao@ciac.jl.cn) (L. Gao).

films. The Phen was selected as ligand owing to the good compatibility of the aromatic Phen, which could increase the doped content of cerium dioxide in polymer matrix. The structure, morphologies, thermal and mechanical properties were studied in detail via different testing methods.

## 2. Experimental

### 2.1. Materials

Pyromellitic dianhydride (PMDA, 99%) and 4,4'-oxydianiline (ODA, 99%) were purchased from Shanghai Chemical Reagents Company and were purified by sublimation under vacuum. *N,N*-Dimethylacetamide (DMAc, 99.5%) was purified by distillation over phosphorus pentoxide and stored over 4 Å molecular sieves. Cerium(III) nitrate hexahydrate and 1,10-phenanthroline (Phen) were used as received. Other chemical reagents were used without purification.

### 2.2. Synthesis of polyamic acid (PAA)

PAA from PMDA and ODA was synthesized by one-step process in DMAc. ODA (4.00 g, 20 mmol) was dissolved in the dry DMAc with stirring and PMDA (4.36 g, 20 mmol) was added in ODA solution at room temperature. After the reaction mixture was stirred for 24 h, a 10 wt% solution of PAA in DMAc was obtained. Intrinsic viscosities of the resulting polyamic acid were measured as 1.92 dL/g in DMAc at 30 °C, indicating the obtained PAA have high molecular weight.

### 2.3. Synthesis of rare earth complex $Ce(Phen)_3 \cdot 3NO_3^-$

Phen 1.62 g (9 mmol) was dissolved in 30 mL of 95% ethanol, and 1.302 g of  $Ce(NO_3)_3 \cdot 6H_2O$  (3 mmol) in 15 mL of 95% ethanol was added in the above solution at 60 °C under stirring. The reaction solution was then refluxed for 3 h and cooled. The yellow crystals were collected by filtration and washed with ethanol and water. Finally, the rare earth complex of cerium as yellowy solid was obtained under the reduced pressure at 80 °C for 10 h. Yield 85%; IR spectrum ( $cm^{-1}$ ): 3064, 1628, 1600, 1481, 1297, 1028, 844, 725;  $^1H$  NMR (DMSO- $d_6$ , 500 MHz):  $\delta$  7.77 (s, 2H), 8.04 (s, 2H), 8.5 (d, 2H), 9.08 (s, 2H); Anal. Calcd for C, 49.90%; H, 2.71%; N, 14.55%; Ce, 16.17%. Found: C, 49.32%; H, 2.19%; N, 14.22%; Ce, 16.54%.

### 2.4. Preparation of composite films

Different weight percentage of rare earth complex was added into the PAA solution and the mixture was stirred for 2 h to form homogeneous solution. Then the viscous solution was cast on a glass plate and dried on a hot plate at 60 °C for 12 h, followed by a step thermal imidization process (0.5 h each at 100, 150, 200, 250 °C, finally at 300 °C for 2 h).

## 2.5. Characterization

Intrinsic viscosities of the polyamic acid were determined at 30 °C with an Ubbelodhe viscometer and the concentration was 0.5 g/dL in DMAc. FTIR spectra were recorded on a Nicolet AVATAR360 FTIR spectrometer.  $^1H$  NMR spectra were obtained from an AVANCE 500 MHz Bruker spectrometer in DMSO- $d_6$  solution. Thermogravimetric analyses (TGA) were obtained in air with a Perkin–Elmer TGA-2 thermogravimetric analyzer. For the nonisothermal TGA measurement, the heating rate is 20 °C/min and the isothermal TGA was performed at 300 °C for 2 h. The glass transition temperature of composite films was measured on a dynamic mechanical thermal analyzer (DMTA) used film samples (length: 10 mm). The run conditions were conducted at a frequency of 1 Hz and a heating rate of 3 °C/min from 40 to 500 °C in a tensile mode (strain: 0.1%, initial static force: 0.2 N, static > dynamic force by 10.0%, minimum static force: 0.01 N, maximum autotension displacement: 3.0 mm). The tensile measurements were carried out on an Instron model 1122 at room temperature. X-ray photoelectron spectroscopy (XPS) was measured by VG ESCALAB MKII spectrometer. The wide-angle X-ray diffraction (WAXD) measurements were undertaken on a Rigaku max 2500 V PC X-ray diffractometer with Cu  $K\alpha$  radiation (40 kV, 200 mA) with a scanning rate of 2°/min from 5° to 50°. The morphologies of fractured surfaces of composite films were studied with an XL-30 ESEM FEG Scanning Electron Microscope (FEI COMPANY).

## 3. Results and discussion

### 3.1. Characterization of cerium complex

The cerium complex was synthesized from  $Ce(NO_3)_3 \cdot 6H_2O$  and Phen with a molar ratio of 1:3. The complex is easy to dissolve in polar solvents, such as DMAc, DMF, dimethyl sulfoxide (DMSO), etc. Fig. 1 shows the FTIR

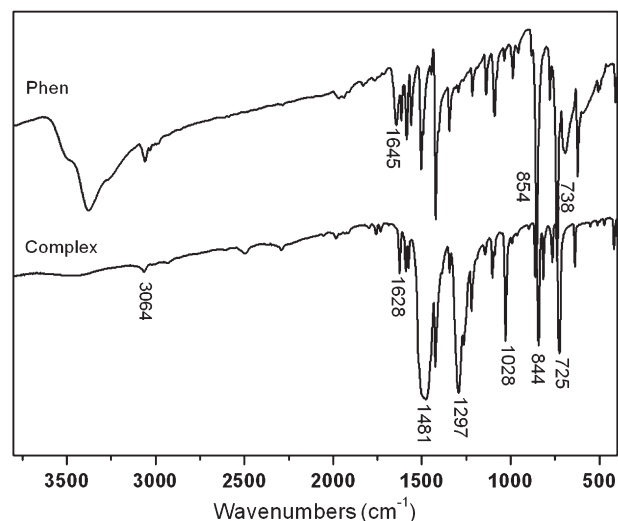


Fig. 1. FTIR spectra of  $Ce(Phen)_3$  and Phen.

spectra of the obtained cerium complex and Phen. The stretching vibration of Phen at  $1645\text{ cm}^{-1}$  and the bent vibrations at  $854$  and  $738\text{ cm}^{-1}$  were shifted to  $1628$ ,  $844$ , and  $725\text{ cm}^{-1}$ , indicating that Phen has coordinated with the cerium ion. In addition, another evident change in FTIR spectra was the disappearance of absorption peak at  $3388\text{ cm}^{-1}$  related to absorption of water as Phen and cerium ion form complex. TGA analysis showed that the complex does not contain crystalline water (Fig. 2a).  $^1\text{H NMR}$  spectrum of cerium complex confirmed the existence of characteristic peaks of Phen at  $\delta = 9.07$ ,  $8.50$ ,  $7.99$  and  $7.76\text{ ppm}$  (Fig. 3). It was found that when Phen coordinates with cerium ion to form complex, the peak of ligand Phen at  $\delta = 9.10$  ( $1\text{H}_{\text{C}=\text{N}}$ ) broadens and shifts to high field ( $\delta = 9.06$ ) owing to the change of chemical circumstance. The C, H, N and Ce contents of the complex determined by elemental analysis were  $49.32\%$ ,  $2.19\%$ ,  $14.22\%$  and  $16.54\%$ , respectively, which is well in accordance with the calculated values for the structure of new cerium complex  $\text{Ce}(\text{Phen})_3 \cdot 3\text{NO}_3^-$ . The thermal property of complex was studied by TGA (Fig. 2). The nonisothermal curve (Fig. 2a)

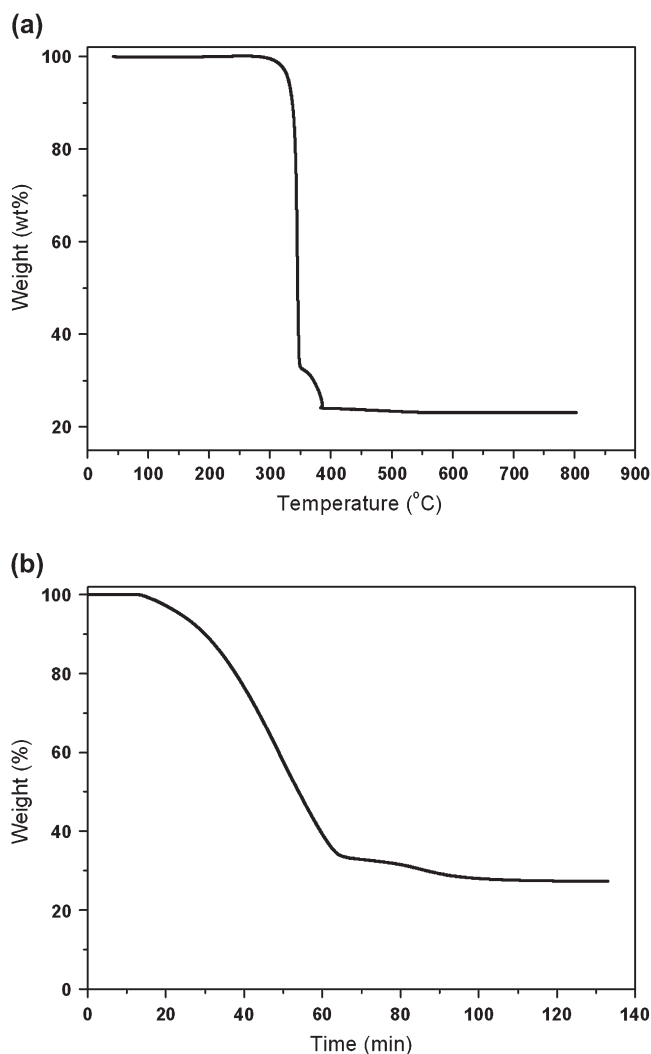


Fig. 2. Nonisothermal (a) and isothermal (b) TGA curves of complex of  $\text{Ce}(\text{Phen})_3$ .

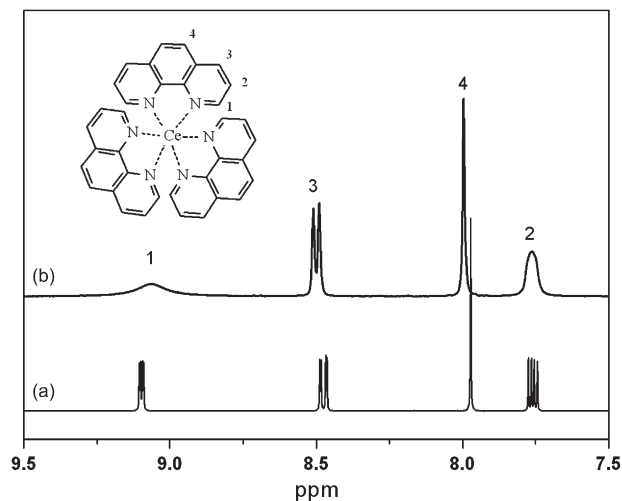


Fig. 3.  $^1\text{H NMR}$  spectra of (a) Phen and (b)  $\text{Ce}(\text{Phen})_3$ .

of cerium complex revealed a main thermal decomposition process at  $320\text{--}340\text{ }^\circ\text{C}$  and a minor shoulder of weight loss at  $350\text{--}390\text{ }^\circ\text{C}$ . However, the isothermal curve (Fig. 2b) showed that the cerium complex has begun to decompose above  $300\text{ }^\circ\text{C}$  after 15 min and almost completely decomposed after 65 min. This result indicated that the cerium complex in polyimide may form  $\text{CeO}_2$  at the thermal imidization conditions (see following discussion).

### 3.2. Characterization of nanocomposite films

Fig. 4 shows FTIR spectra of the hybrid films. The absorption peaks at  $1776$ ,  $1709$ ,  $1370$ ,  $1113$  and  $719\text{ cm}^{-1}$  are contributed to characteristic absorption of imide groups in PI and hybrid films. The characteristic peak at  $1650\text{ cm}^{-1}$  for PI precursor (PAA) disappears, indicating that the imidization reaction is complete [14,25]. Unfortunately, the absorption of  $\text{CeO}_2$  cannot be observed due to its weak absorption intensity in IR spectrum. So all the spectra of both PI and hybrid films

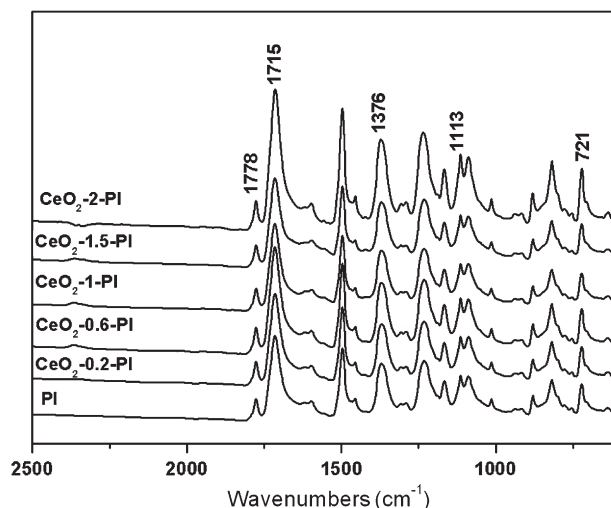


Fig. 4. FTIR spectra of PI hybrid films.

with different complex contents present the similar spectrum profile.

To testify the existence of  $\text{CeO}_2$  in PI films, the XPS was used to characterize the hybrid films. Fig. 5 shows the  $\text{Ce}3d$  XP spectrum of the hybrid with 2 wt% cerium dioxide complex. The photoelectron peaks of  $\text{Ce}3d_{5/2}$  and  $\text{Ce}3d_{3/2}$  appear at the binding energies of 882.5, 885.8 eV and 900.9, 904.5 eV, respectively [26]. This result confirms that the cerium complex is incorporated into PI to form  $\text{CeO}_2$ .

The XRD patterns of cerium complex and hybrid films are shown in Fig. 6. The cerium complex exhibits several sharp diffraction peaks with a strong peak at  $2\theta = 12.4^\circ$ . However, no characteristic XRD peaks of pure cerium complex were observed in complex/PI hybrid films. These hybrids give the same broad halo diffraction peak at around  $2\theta = 19^\circ$  as that of the pure PI film, indicating cerium complex has been decomposed to form  $\text{CeO}_2$ . But the characteristic diffraction peaks of  $\text{CeO}_2$  did not be observed. It may be that the peaks of  $\text{CeO}_2$  were overlapped by the peaks of polymer matrix due to the low content of  $\text{CeO}_2$ .

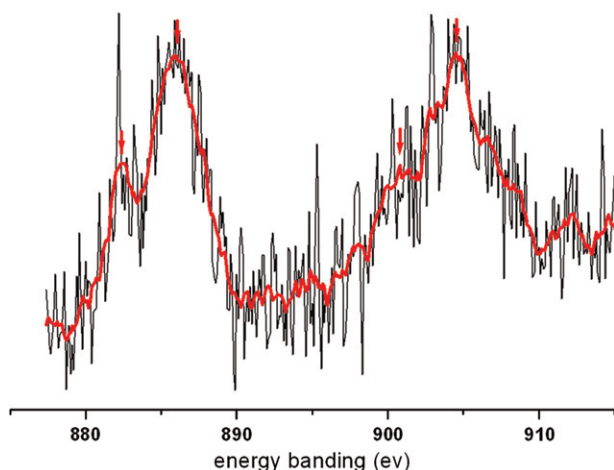


Fig. 5.  $\text{Ce}3d$  XP spectrum of composite films with 10 wt% of complex.

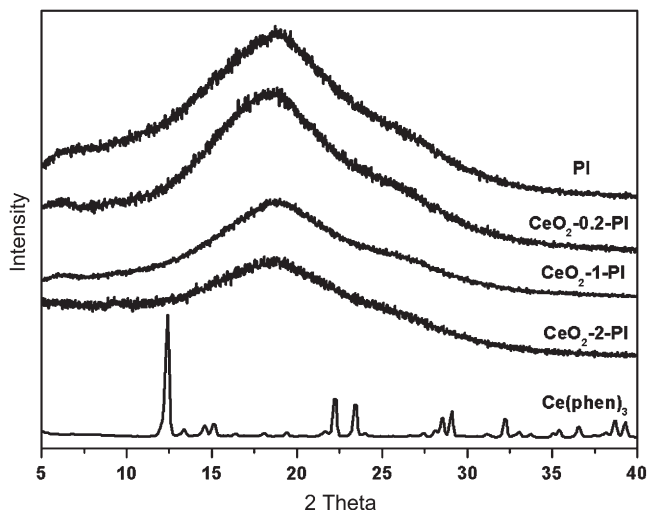


Fig. 6. X-ray diffraction patterns of cerium complex and composite films.

Fig. 7 shows the SEM photographs of the fracture surface of nanocomposite films. It can be clearly seen that the nanoparticles ( $\text{CeO}_2$ ) with a diameter of 40–70 nm distribute uniformly in the polymer matrix for the hybrid films with 0.6 and 2 wt% of cerium dioxide complex. However, the similar nanoparticles cannot be clearly observed in the hybrid sample with low  $\text{CeO}_2$  content (0.2 wt%). This may be that the  $\text{CeO}_2$  content is very low in polymer. In addition, we can also see that the  $\text{CeO}_2$  nanoparticles are imbedded in polymer matrices, indicating that the  $\text{CeO}_2$  has good compatibility and interfacial interaction with polyimide matrix, which favors for the improvement of thermal and mechanical properties of hybrids.

TGA was used to study the thermal properties of the nanocomposite films and the results are listed in Table 1. It can be seen that the thermal stability of composite films with different contents of cerium dioxide ( $T_d = 410\text{--}512^\circ\text{C}$ ) decreases obviously compared with that of pure polyimide. However, we did not find any clear variation rule for composite films with the change of  $\text{CeO}_2$  content. The composite films with 0.2 and 2 wt%  $\text{CeO}_2$  exhibit lower thermal stability, while the composite film with 1 wt%  $\text{CeO}_2$  has the relative high stability. At present, we have not known the detailed reason. But it is clear that the introduction of  $\text{CeO}_2$  from cerium complex with Phen in PI matrix will decrease the thermal stability of composites.

The glass transition temperatures of nanocomposite films were determined by DMTA (Fig. 8). The DMTA curves ( $\tan \delta$ ) of different composite films show a primary glass transition temperature (388–406  $^\circ\text{C}$ ) corresponding to PI matrix (Table 1), and the  $T_g$  of the composite films increases with increasing  $\text{CeO}_2$  content in comparison with the pure PI. Meanwhile, the  $\tan \delta$  breadth is wider and the  $\tan \delta$  damping decreases with the increasing of  $\text{CeO}_2$  content. It has also been observed that as the  $\text{CeO}_2$  content reaches above 1.5 wt%, the peaks of  $\tan \delta$  become an evenly platform and then the curves increase rapidly above 420  $^\circ\text{C}$ , so it is difficult to determine the  $T_g$  values of hybrids in the testing temperature range. This thermal transition behavior of the composite samples should be an indicative of the cooperative nature of the relaxation process of the polymer chains. As the  $\text{CeO}_2$  nanoparticles are formed in PI, the free volume of the polymer will reduce, and the interaction of the nanoparticles with polymer molecules will further restrict the motion of polymer chain segments [27]. Especially, for the composite samples with high  $\text{CeO}_2$  loading, this interaction between particles and polymer becomes stronger and even makes the  $T_g$  disappear. This phenomenon was also observed in other organic/inorganic hybrid systems [28–30].

The mechanical properties of the composite films are listed in Table 1. The modulus of the composite films increases with increasing  $\text{CeO}_2$  content, while the elongation at break decreases obviously for the composite films with above 1 wt% of  $\text{CeO}_2$  content. There is a maximum value for the tensile strength as 0.6 wt% of cerium dioxide is incorporated in PI. It can be seen that the introduction of small amount of cerium dioxide (<1 wt%) leads to the reinforcement of the



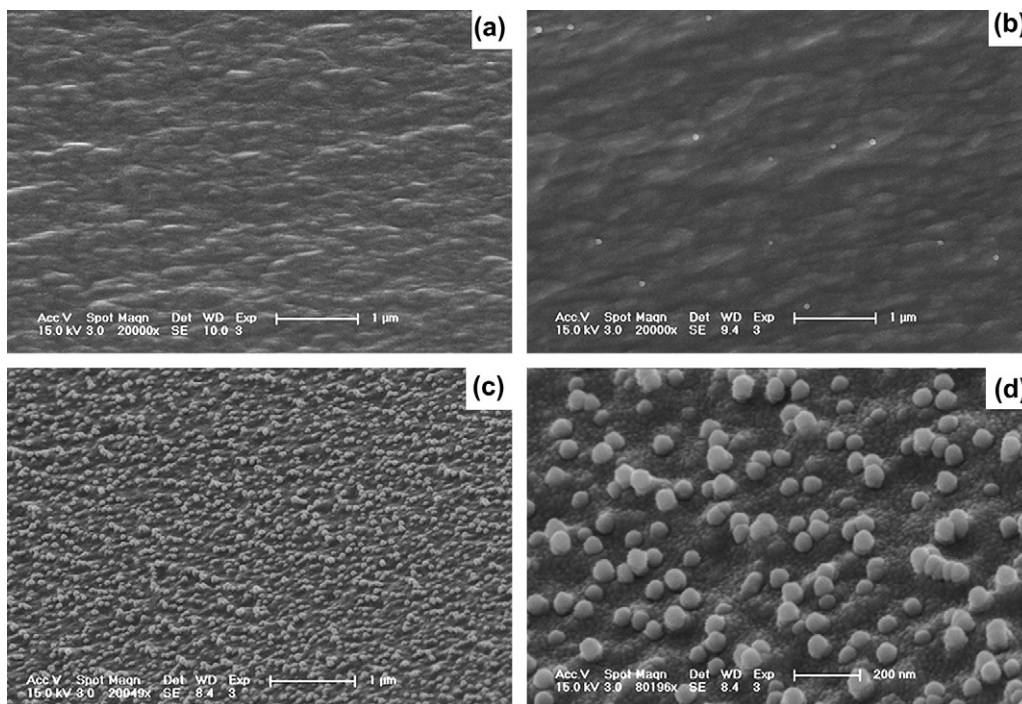


Fig. 7. SEM images of nanocomposite films: (a) CeO<sub>2</sub>-0.2-PI, (b) CeO<sub>2</sub>-0.6-PI, (c) CeO<sub>2</sub>-2-PI, and (d) magnification image of (c).

Table 1  
Some properties of nanocomposite films

Sample <sup>a</sup>	Modulus (MPa)	Tensile strength (MPa)	Elongation (%)	$T_d^b$ (°C)	$T_g^c$ (°C)
PI	2200	135	83	556	388
CeO <sub>2</sub> -0.2-PI	2270	152	76	410	396
CeO <sub>2</sub> -0.6-PI	2350	170	70	470	398
CeO <sub>2</sub> -1-PI	2570	155	50	512	406
CeO <sub>2</sub> -1.5-PI	3150	121	7.5	482	—
CeO <sub>2</sub> -2-PI	3300	108	4.2	433	—

<sup>a</sup> The numbers in the CeO<sub>2</sub>-*x*-PI represent the theoretical content of CeO<sub>2</sub> from complete decomposition of cerium complex in PI.

<sup>b</sup> 5 wt% decomposition temperature.

<sup>c</sup> Glass transition temperature of composite films obtained by DMTA.

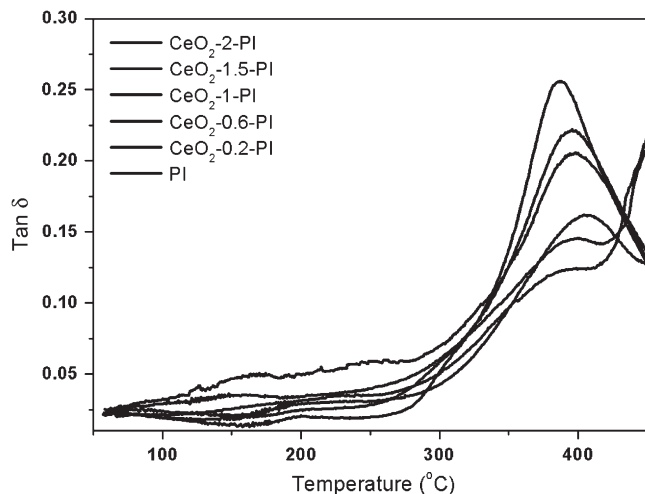


Fig. 8. DMTA curves (tan  $\delta$ ) of nanocomposite films.

mechanical properties of composite films, and at the same time the composite films maintain good flexibility. The well interfacial interaction between PI matrix and CeO<sub>2</sub> particles as well as the uniform nanophase distribution in composite films has a positive effect on the improvement of mechanical properties of the composite films. The DMTA result is in accordance with that of the static mechanical test. Fig. 9 shows the curves of the storage modulus measured by DMTA for the composite films. When the content of CeO<sub>2</sub> in the films increases, the films exhibit higher values of storage modulus on the whole.

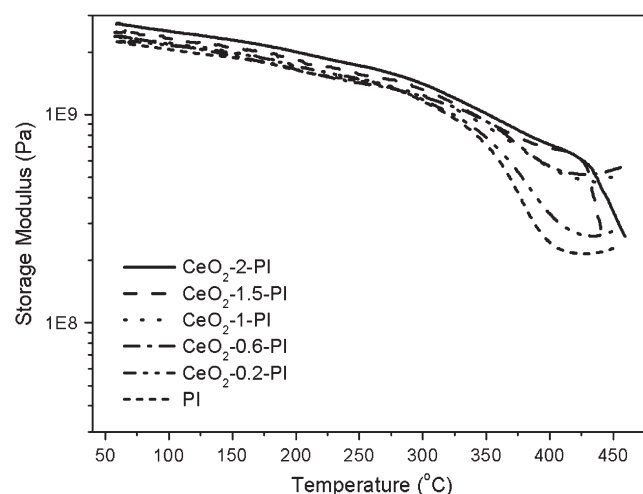


Fig. 9. DMTA curves (storage modulus) of nanocomposite films.

#### 4. Conclusion

The CeO<sub>2</sub>/PI nanocomposite films were prepared from polyamic acid and a new cerium complex with Phen ligand. The cerium dioxide as 40–70 nm particles from decomposed cerium complex distributes homogeneously in polyimide matrix. The strong interaction between CeO<sub>2</sub> nanoparticles and polyimide matrix brings obvious effect on the thermal transition behavior and mechanical properties of composites, although the thermal stability decreases. Thus, to improve the properties of composites, it is important to control the nanophase uniform dispersion in polymer matrix as well as the interaction of different hybrid components.

#### Acknowledgements

The authors would like to acknowledge the financial support of the National Natural Science Foundation of China (No. 50333030).

#### References

- [1] Komarneni S, Parker JC, Thomas GJ. Nanophase and nanocomposite materials. Pittsburgh, PA: Materials Research Society; 1993.
- [2] Caseri W. *Macromol Rapid Commun* 2000;21:705.
- [3] Sanchez C, Julián B, Belleville P, Popall M. *J Mater Chem* 2005; 15:3559.
- [4] Schmidt G, Malwitz MM. *Curr Opin Colloid Interface Sci* 2003;8:103.
- [5] Beecroft LL, Ober CK. *Chem Mater* 1997;9:1302.
- [6] Fischer H. *Mater Sci Eng* 2003;C23:763.
- [7] Lü C, Cui Z, Guan C, Guan J, Yang B, Shen J. *Macromol Mater Eng* 2003;288:717.
- [8] Ahmad Z, Mark JE. *Chem Mater* 2001;13:3320.
- [9] Sroog CE. *Prog Polym Sci* 1991;16:561.
- [10] Ghosh MK, Mittal KL. *Polyimides: fundamentals and applications*. New York: Marcel Dekker; 1996.
- [11] Hasegawa M, Horie K. *Prog Polym Sci* 2001;26:259.
- [12] Park HB, Kim JH, Kim JK, Lee YM. *Macromol Rapid Commun* 2002; 23:544.
- [13] Cornelius CJ, Marand E. *Polymer* 2002;43:2385.
- [14] Musto P, Ragosta G, Scarinzi G, Mascia L. *Polymer* 2004;45:1697.
- [15] Chiang PC, Whang WT. *Polymer* 2003;44:2249.
- [16] Tong Y, Li Y, Xie F, Ding M. *Polym Int* 2000;49:1543.
- [17] Jiang LY, Leu CM, Wei KH. *Adv Mater* 2002;14:426.
- [18] Lan T, Kaviratna PD, Pinnavaia TJ. *Chem Mater* 1994;6:573.
- [19] Thompson CM, Herring HM, Gates TS, Connell JW. *Compos Sci Technol* 2003;63:1591.
- [20] Espuchea E, Davida L, Rochasb C, Afeldc JL, Comptonc JM, Thompsonc DW, et al. *Polymer* 2005;46:6657.
- [21] Southward RE, Thompson DS, Thornton TA, Thompson DW, Clair St AK. *Chem Mater* 1998;10:486.
- [22] Thompson DS, Thompson DW, Southward RE. *Chem Mater* 2002;14:30.
- [23] Bian LJ, Qian XF, Yin J, Lu QH, Liu L, Zhu ZK. *Polymer Testing* 2002;21:841.
- [24] Bian LJ, Qian XF, Yin J, Zhu ZK, Lu QH. *J Appl Polym Sci* 2002; 86:2707.
- [25] Qiu W, Luo Y, Chen F, Duo Y, Tan H. *Polymer* 2003;44:5821.
- [26] Natile MM, Boccaletti G, Glisenti A. *Chem Mater* 2005;17:6272.
- [27] Lee LH, Chen WC. *Chem Mater* 2001;13:1137.
- [28] Bershtein VA, Egorova LM, Yakushev PN, Pissis P, Sysel P, Brozova L. *J Polym Sci Part B Polym Phys* 2002;40:1056.
- [29] Hsu SC, Whang WT, Hung CH, Chiang PC, Hsiao CY. *Macromol Chem Phys* 2005;206:291.
- [30] Chen Y, Zhou S, Yang H, Wu L. *J Appl Polym Sci* 2005;95:1032.